Cross-Section Measurement for Z Boson Decays using ATLAS
Third Year Lab Report

Amrit Bath: 10899510
Department of Physics and Astronomy, University of Manchester
(Experiment performed in collaboration with Jade Huang: 10639013)
(Dated: December 18, 2024)

This report investigates the Z boson cross section using data from the ATLAS detector. This was calculated via Monte Carlo simulations and selection cuts applied at invariant mass of 77–120 GeV, transverse momentum > 17 GeV, and cuts on isolation variables, giving a value of $\sigma_{(\mathrm{Zee})} = 1.987 \pm 0.002_{(\mathrm{stat})} \pm 0.007_{(\mathrm{sys})} \pm 0.034_{(\mathrm{lumi})}$ nb.

1. INTRODUCTION

The Standard Model is a framework which describes the four fundamental forces. Within this model, the electroweak interaction unifies electromagnetic and weak forces, mediated by W and Z bosons [1]. Its production and decay properties enable testing of the Standard Model's predictions. It also allows analysis of current and future theories such as super symmetry, ultimately leading to a more unified theory of particle physics. The strong force is also important, as it dictates proton structure and binds quarks together [2]. A Toroidal LHC Apparatus, or ATLAS is a multi-component detector designed to measure particles with exceptional precision. Its key systems, including the inner tracker, calorimeters, and muon spectrometer, allow identification and reconstruction of particles emerging from high-energy collisions [3]. The ATLAS detector at CERN's Large Hadron Collider enables such studies by using Z boson centre-of-mass energy, $\sqrt{s} = 13TeV$, and analysing proton-proton collisions [4]. ROOT framework is an advanced object-oriented toolkit for efficient data processing in high-energy physics research, and is also important to consider when using ATLAS [5]. A possible decay of the Z boson is into a lepton and anti-lepton pair, such as an electron and positron. These decays are particularly valuable for analysis due to the clean and detectable signature they leave in the detector.

2. THEORY

2.1. Z Boson Decay Channels

Z bosons are massive with mass $91GeV/c^2$ [1]. They can decay into two leptons, of opposite flavour due to their neutral charge, for example, an electron positron pair or a muon and anti-muon pair. A Feynman diagram of this decay can be seen in Figure 1.

2.2. Background Processes

Many other phenomena can also produce leptonic pairs, such as the decay of tau particles into electrons.

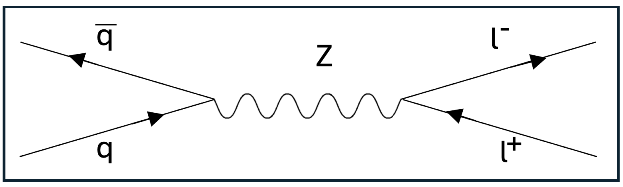

FIG. 1. shows the process of a Z boson being produced from a quark anti-quark pair, and producing a lepton and anti-lepton as a result.

This can influence the analysis of Z boson decay to electron positron pairs, due to them being indistinguishable [3]. To mitigate this, we must use event selection criteria [6]. Part of these complications arise from the inherent structure of protons, which are composed of quarks and gluons, bound by the strong force. During collisions, these constituents interact via hard scatter processes, which are high-energy interactions between quarks or gluons in a collision mediated by gluon exchanges. Gluons can radiate and split into quark anti-quark pairs, or interact with other gluons, producing more particles. This results in jets, which are streams of particles that form when quarks and gluons combine into hadrons. These jets significantly contribute to the complexity produced by collision events. They generate a cluster of particles and energy deposits that obscure the clean signals from Z boson decays [7]. Additionally, low-energy gluon radiation and secondary interactions from surrounding particles further complicate the environment, creating overlapping events and pile-up effects in the detector.

2.3. Finding the Cross-Section

The cross section σ is an important quantity, describing the probability of a specific interaction occurring during a particle collision [8]. The cross section is calculated using

$$\sigma = \frac{N_{\mathrm{selected}} - N_{\mathrm{background}}}{\mathcal{L}\,\epsilon} \tag{1}$$

where N denotes the integral number of events, and the numerator, $N_{\mathrm{selected}} - N_{\mathrm{background}}$ can be defined as N_{signal}, this isolates the signal events by subtracting background contributions from the total observed events. The integrated luminosity, $\mathcal{L}$, is the intensity of proton beams and represents the total number of proton-proton collisions that occurred during the data collection period. The higher the integrated luminosity, the greater the number of collisions. This value is given as $10.064fb^{-1}$, with an uncertainty of $\pm 1.7\%$. ϵ denotes the efficiency.

2.4. The Efficiency

The efficiency, ϵ, corrects for detector and analysis inefficiencies, scaling up the value to represent the entire system [4], it can be found using the equation

$$\epsilon = \frac{N^{\mathrm{selected}}_{Z\to l^+l^-}}{N^{\mathrm{total}}_{Z\to l^+l^-}} \tag{2}$$

where $N^{\mathrm{selected}}_{Z\to l^+l^-}$ is the number of $Z \to l^+l^-$ processes that pass the selection cuts in the Monte Carlo (MC) simulation, and $N^{\mathrm{total}}_{Z\to l^+l^-}$ is the total number of events which are expected to occur in the collider.

2.5. The Invariant Mass

The invariant mass represents the mass of a system of particles, independent of its reference frame [9]. It is calculated from particle energy and momentum, and is useful in identifying particles such as Z bosons and identifying interactions. The invariant mass of two particles is particularly useful for distinguishing signal and background events by identifying characteristic peaks corresponding to specific particle decays. The invariant mass, m_{ll}, for a lepton anti-lepton system can be expressed as

$$m_{\ell\ell} = \sqrt{2p_{T1}p_{T2}\left(\cosh(\eta_1 - \eta_2) - \cos(\phi_1 - \phi_2)\right)}. \tag{3}$$

Here, p_{T1} and p_{T2} represent the transverse momenta of the two leptons. η_1 and η_2 are their pseudorapidities, and the azimuthal angles of the leptons in the transverse plane are given by ϕ_1 and ϕ_2. The invariant mass distribution is expected to peak at the mass of the Z boson. Plotting this means we can investigate the signal corresponding to Z boson decays.

2.6. Other Important Variables

In addition to invariant mass, variables such as ptcone30 and etcone20 are crucial in the analysis. The variable ptcone30 measures the scalar sum of transverse momenta of charged particle tracks within a cone of half-width 0.3 in ΔR around the lepton. Tracks represent reconstructed trajectories of charged particles in the detector, and a low ptcone30 value indicates am isolated lepton. etcone20 is similar, and evaluates the sum of transverse energy deposits within a smaller cone $\Delta R = 0.2$ around the lepton in the calorimeter. Rather than tracking individual particles, it averages energy deposits, incorporating corrections to account for detector effects and overlapping events, leading to a broader distribution [10].

3. EXPERIMENTAL ANALYSIS

3.1. Data Collection and Initial Setup

Data was accessed using the ATLAS Open Data platform through a remote virtual machine setup. The experimental framework involved processing real and MC simulated datasets. MC datasets, such as `Zee` and `Zmumu`, represent events involving Z boson decays to electron-positron and muon-antimuon pairs, respectively. The real dataset, `2lep`, included all relevant physics processes, providing a basis for comparison.

3.2. Event Selection and Filtering

To identify events consistent with $Z \to e^+e^-$ decays, selection criteria were applied. Events were required to contain exactly two leptons. To do this, the selection was restricted to electrons (lepton type 11), and the two leptons were required to have opposite charges to each other, in order to match the expected signature. Numerical cuts were determined by comparing stacked plots of individual background processes with the dataset. This helped identify regions most influenced by background. These regions were then excluded to improve the analysis. An example of an area contaminated with large background processes can be seen Figure 2, here, the main source of background comes from process $t\bar{t}$. Through an in depth analysis of these background processes, cuts can be made for each variable being considered. Figures 3 and 4 show a comparison of the invariant mass, and the MC simulation for $Z \to e^+e^-$ before and after the cuts had been made on our data and simulations, respectively.

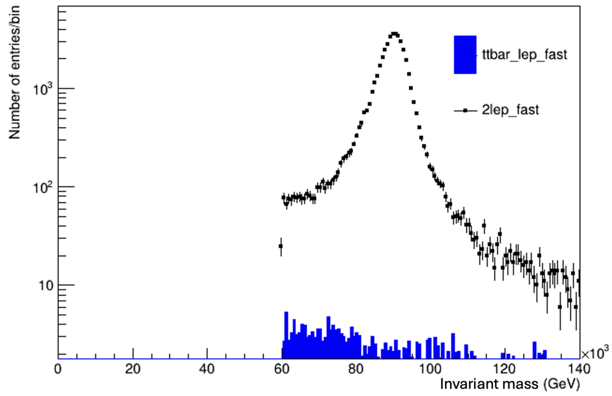

FIG. 2. This stacked logarithmic plot shows the dataset and $t\bar{t}$ MC distribution.

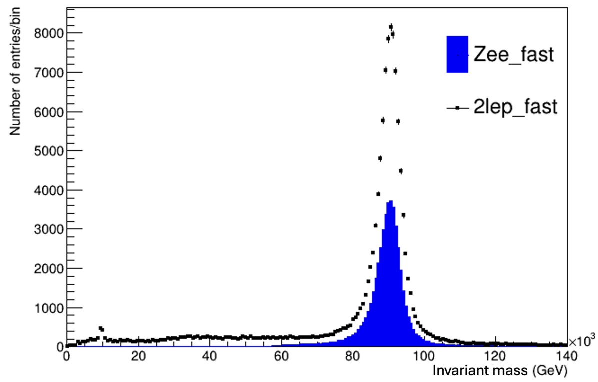

FIG. 3. Stacked histogram of the dataset and MC simulation, prior to any cuts being applied.

3.3. Monte Carlo Deviations

The simulation data sets provided a reference for validating real data. Overlaying the invariant mass distribution from real data with MC simulations revealed strong alignment for invariant masses above 60 GeV, where the MC simulation began. Below 60 GeV, there were unaccounted for background processes not in-

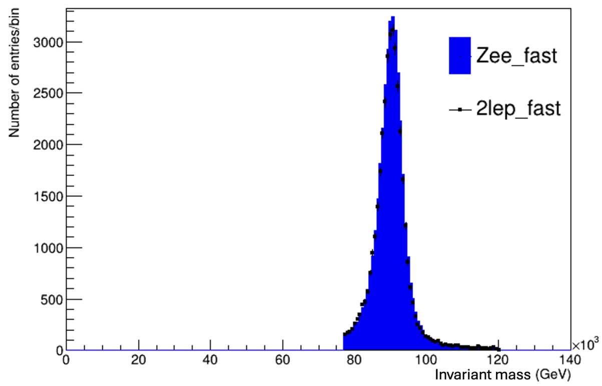

FIG. 4. Stacked plot of the dataset with the MC simulation, after applying final cuts.

cluded in the simulations, which could effect analysis, therefore selection cuts were applied to remove these background processes. Additionally, smudging effects due to the detector would need to be considered.

3.4. Refinements and Final Cuts

Our final conditions specified electron-positron pairs being produced, with numerical cuts shown in table I. After further analysis, we reproduced our plots using

TABLE I. Final Selection Cuts for $Z \to e^+e^-$ Analysis

Condition	**Range/Value**
Invariant Mass Range	77–120 GeV
Transverse Momentum (p_T)	> 17 GeV
`Ptcone[0]`	< 1750 GeV
`Ptcone[1]`	< 2250 GeV
`Etcone[0]`	> -2000 GeV
`Etcone[1]`	> -1800 GeV

the same selection criteria, but investigated opposite-flavour lepton pairs ($Z \to e^+\mu^-$ or $Z \to e^-\mu^+$). This approach provided understanding of the imperfections in the MC models. In a perfectly accurate MC simulation, the presence of opposite-flavour leptons would indicate that all observed processes are background events, with no signal contribution from Z boson decays. However, data revealed non-zero events in this region, suggesting discrepancies between our MC simulations and the real detector environment. This observation highlights the need to refine the modelling of background processes. By calculating a scale factor of about 1.5 to the simulated background events, we could enhance the alignment between the MC predictions and the actual data. This adjustment improves the accuracy of the background estimation, ensuring that our final analysis reflects a more realistic representation of the underlying physics.

4. RESULTS AND ERROR ANALYSIS

4.1. Error Analysis

Error analysis focused on three sources of uncertainty, statistical, systematic and luminosity. The luminosity has a standard error of ±1.7%. Statistical uncertainties arose from the limited number of events, this fluctuates due to the random processes in particle collisions. These uncertainties were quantified using the propagation of errors. The statistical uncertainty in N_{selected} follows a Poisson distribution and is given by $\sqrt{N}$. For the background processes, the statistical uncertainty is calculated as the integral value multiplied by $\sqrt{\text{N\_entries}}/\text{N\_entries}$. To determine the total statistical uncertainty, contributions from different sources are combined in quadrature.

Systematic uncertainties stemmed from detector calibration, efficiency modelling and mismodeling in the MC simulations. With perfect MC simulations, the cuts taken would still have reproduced the same cross-section. We could therefore vary our cuts slightly, and investigate the impact of this on the cross section. Taking the standard deviation of these variations allows us to quantify our systematic error.

4.2. Obtained Cross Section Result and Literature Comparison

After completing our analysis we can compare our result to the literary value and evaluate that our findings were consistent. This confirms the accuracy of the event selection used, background subtraction, and systematic uncertainty evaluation applied during the study. [8]. These were found to be:

$$\sigma_{(\text{Zee})} = 1.987 \pm 0.002_{(\text{stat})} \pm 0.007_{(\text{sys})} \pm 0.034_{(\text{lumi})}\ \text{nb}$$

$$\sigma_{(\text{literature})} = 1.981 \pm 0.007_{(\text{stat})} \pm 0.038_{(\text{sys})} \pm 0.042_{(\text{lumi})}\ \text{nb}$$

5. CONCLUSION

This analysis measures the cross-section for $Z \to e^+e^-$ decays using ATLAS data, successfully isolating signal events through event selection criteria and Monte Carlo simulations. Selection cuts and invariant mass distributions enabled signal identification, providing a cross-section consistent with literature, confirming the methodology's accuracy and the ATLAS detector's reliability. Background scale factors refined Monte Carlo models, exposing discrepancies requiring further investigation. Statistical and systematic uncertainties were thoroughly analysed, emphasising the need for further investigation into Monte Carlo models. Future work could explore correlated background variables and variations in cut positioning.

[1] Science, Discovery of the z boson: A significant advancement in particle physics (1990), accessed: 15 December 2024.

[2] M. Physics, Measurements of z boson properties in recent experiments (2023), accessed: 15 December 2024.

[3] ScienceDirect, Analysis of z boson production and its applications in high-energy physics (2019), accessed: 15 December 2024.

[4] A. Collaboration, Measurements of the production cross section of a z boson in association with jets in pp collisions at $\sqrt{s} = 13$ tev with the atlas detector (2017), accessed: 15 December 2024.

[5] A. Collaboration, Performance and calibration of the atlas simulation framework (2012), accessed: 15 December 2024.

[6] A. Collaboration, Event selection services in atlas (2010), accessed: 15 December 2024.

[7] A. Collaboration, Cross-section measurements for the production of a z boson in association with high-transverse-momentum jets in pp collisions at $\sqrt{s} = 13$ tev with the atlas detector (2022), accessed: 15 December 2024.

[8] A. Collaboration, Measurement of $w^{\pm}$ and z-boson production cross sections in pp collisions at $\sqrt{s} = 13$ tev with the atlas detector (2016), accessed: 15 December 2024.

[9] M. J. W. S. a. E.L. Berger, D. DiBitonto, The minimum invariant mass — a technique for heavy quark searches at collider energy (1984), accessed: 15 December 2024.

[10] C. Pizio, Missing transverse energy measurement in atlas detector: First lhc data results and importance for physics study (2010), accessed: 15 December 2024.